

Neutral helium line profiles through the simulation of local interactions

Patrick Tremblay¹, Alain Beauchamp and Pierre Bergeron

Département de Physique, Université de Montréal, C. P. 6128, Succ. Centre-Ville,
Montréal, QC H3C 3J7, Canada

email: patrick@astro.umontreal.ca

Abstract. For the past 25 years, we have been considering the Stark effect for neutral helium lines in DB white dwarfs using the standard Stark broadening theory in both the impact regime (in the center of the lines) and the quasi-static regime (in the wings) for the electrons, while neglecting the effect of ions in motion. Although this is probably a good approximation based on previous theoretical work, the transition between the two regimes for the electrons and the contribution of the ions very near the core might be poorly represented. To better represent these particularities, we report here the results of a new series of simulations that treat the local dynamics and interactions of both electrons and ions around a neutral helium atom. From these simulations, we produce new improved line profiles, which we compare with our previous analytical results.

Keywords. line: profiles, atomic processes, methods: n-body simulations, methods: statistical, techniques: spectroscopic

1. Introduction

There are two general methods for measuring the physical parameters of white dwarf stars. First, the effective temperature (T_{eff}) and surface gravity ($\log g$) can be measured by fitting optical spectra with the predictions of detailed model atmospheres, the so-called spectroscopic technique. Alternatively, the photometric energy distributions can be fitted with synthetic photometry, yielding in this case a measurement of T_{eff} as well as the stellar radius if the distance to the star is known. The mass-radius relation for white dwarfs can then be used to infer all other quantities, and most importantly the stellar mass. In principle, both the spectroscopic and photometric techniques should yield similar results.

Genest-Beaulieu *et al.* (2019) compared the mass distributions of DB stars as a function of effective temperature using both techniques (see their Figure 10). While the photometric mass distribution is well centered around the average mass of $0.6 M_{\odot}$ at all temperatures, the spectroscopic mass distribution shows significant departures from this average mass, which also depend on the range of temperature considered. Genest-Beaulieu *et al.* have invoked several possibilities to account for these discrepancies, including flux calibration issues, line broadening theory, and convective energy transport. In this paper, we explore the possibility that Stark broadening may be responsible for some of the problems, at least at high effective temperatures where the Stark effect dominates.

For instance, we show in Figure 1 our best fit to a very high signal-to-noise spectrum of BPM 17088 (WD 0308–565) obtained with the X-shooter spectrograph at the ESO Very Large Telescope, and provided to us by S. Moehler (private communication). While the overall fit is excellent, the high quality of this optical spectrum reveals some small, but significant discrepancies, in particular in the line cores and in the far wings of some

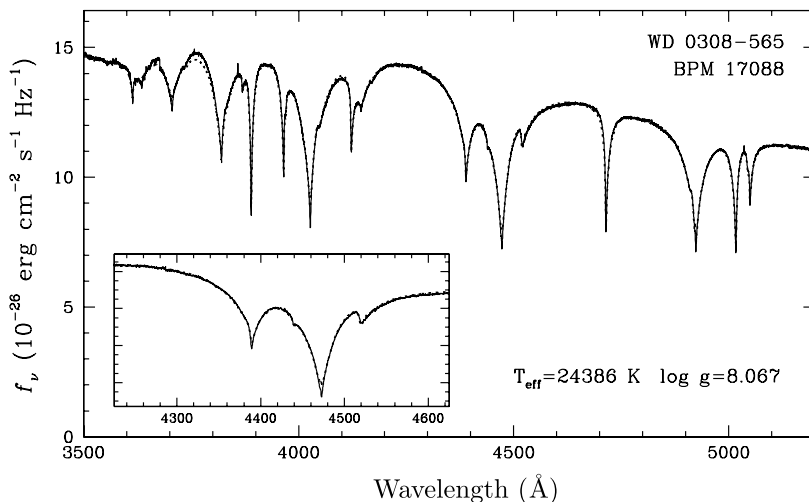


Figure 1. Our best spectroscopic fit (dotted line) to the high-resolution spectrum of the DB white dwarf BPM 17088 (WD 0308-565). The inset is a zoomed-in view near He I $\lambda 4471$.

absorption lines. At this temperature ($T_{\text{eff}} \sim 24,000$ K), however, we cannot completely rule out that the observed discrepancies might be related to some inaccurate treatment of convective energy transport. To disentangle both problems, we feel it is thus necessary to revisit our treatment of the Stark broadening of neutral helium lines.

2. Stark broadening

Stark broadening takes place in the presence of electric fields produced by charged particles in the emitter environment. Strong electric fields present in the photospheric regions of DB white dwarfs produce two effects: the atomic energy levels of the helium atom become a function of the electric field intensity, and the mixing of the different neighboring atomic levels leads to transitions that are normally not allowed by the selection rules for electric dipole transitions. In a few cases, these transitions may be observed as forbidden components. The $2P^3 - 4D^3$ $\lambda 4471$ transition is the classic example often used to describe Stark broadening of a neutral helium line. Figure 2 displays the behavior of the upper levels involved in the He I $\lambda 4471$ Stark-broadened profiles ($m=0$ only, assuming a field along the z direction). For the sake of simplicity, we assume here that the lower levels are unaffected by the electric field, and we investigate the behavior of the upper levels only. As observed in the figure, the energy of the perturbed upper levels is highly dependent on the field intensity, in a non-linear way. The final profile is an average over every possible temporal sequence of local electric fields that is consistent with the distribution of dynamic perturbers in the vicinity of the emitting helium atom.

Our former modeling of Stark broadening was based on the standard theory, as developed by [Barnard *et al.* \(1969\)](#), and applied by [Beauchamp \(1995, 1997\)](#) in the context of DB white dwarfs. Within this framework, the ions are considered at rest but in various static configurations — the so-called quasi-static regime. In contrast, the broadening due to the much faster electrons is described by the impact approximation in the line cores, and by the one-perturber approximation in the line wings ([Baranger 1962](#)), the latter of which converges to the quasi-static regime. Effects due to perturbing ions and electrons are treated differently within this theoretical framework.

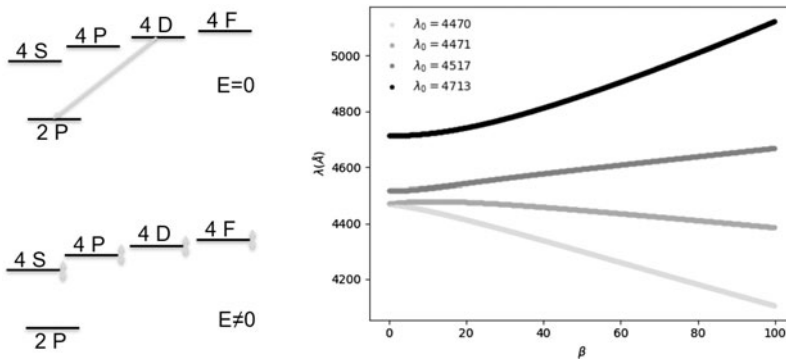


Figure 2. Left: Energy level diagrams in the absence (top) and presence (bottom) of an electric field. Right: Wavelengths of the transitions between perturbed $4S^3$ to $4F^3$ upper levels and the unperturbed $2P^3$ lower level as a function of the normalized electric field strength $\beta = F/F_0$, where F_0 is the normal field strength for an electron density of $N_e = 10^{16} \text{ cm}^{-3}$.

3. An improved approach

Our goal here is to improve these line profile calculations using well-established simulation techniques developed by Gigosos *et al.* (1996, 2014), which treat the effects of dynamic ions and electrons in a unified way. The core of the method consists in generating spherical simulation spaces that reproduce the dynamical environment of the emitter. Each simulation space is defined in the emitter referential, that is, a static emitter is placed at the center of each simulation space, and the perturber velocity follows a Maxwell distribution parameterized by the temperature and the reduced mass of the emitter-perturber pair. For a given temperature and electron number density, the radius of the simulation space is defined as the distance at which the perturbers contribution to the electric field at the emitter position becomes negligible, as described by a Debye-screened potential. Ions and electrons are randomly distributed assuming an electrically neutral plasma, and moving along classical trajectories, which are straight lines for a neutral emitter. The number of perturbers in the simulation volume is allowed to vary, as proposed by Hegerfeldt *et al.* (1988). The set of electric field intensities generated by this process approximately follows the statistical distributions from Hooper (1968).

The physical environment described above allows the electric field to vary both in amplitude and orientation depending on the location of the perturbers. This variation is different for each simulation space, and can thus have different behaviors. For instance, if one or several perturbers pass near the emitter, the field will vary rapidly, as opposed to the case when they are relatively far from the emitter, in a region where the field vector will remain mostly constant. From these simulations, a given line profile can be computed by following these steps:

- A time sequence of 50,000 electric field vectors is extracted for each simulation space.
- The energy of the perturbed levels is computed for each electric field.
- The autocorrelation function, as defined by Griem (1974), is calculated for each simulation space.
- An arithmetic average of the autocorrelation functions obtained amongst 25,000 simulation volumes is performed. The end result is a representation of the line profile in the time domain.
- A Fourier transform is applied to the averaged autocorrelation function to obtain the line profile, in the frequency domain.

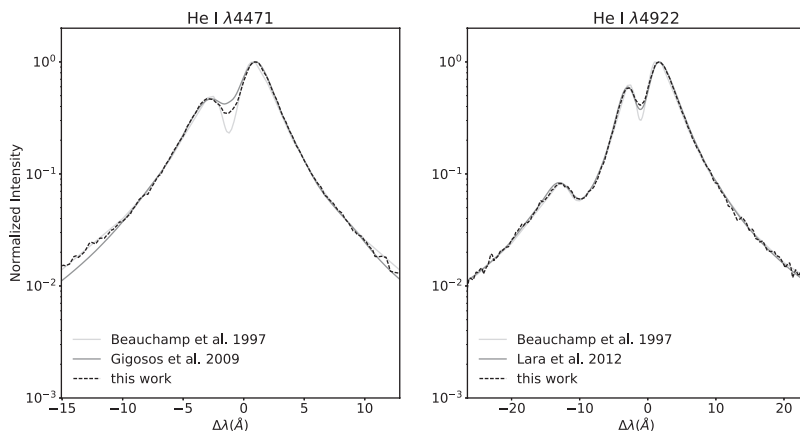


Figure 3. He I $\lambda 4471$ (left panel) and $\lambda 4922$ (right panel) line profiles obtained from our simulations compared to the work of [Beauchamp *et al.* \(1997\)](#), [Gigosos *et al.* \(2009\)](#), and [Lara *et al.* \(2012\)](#), for $\lambda 4922$).

4. Test results

Our simulation code has been tested for the He I $\lambda 4471$ and $\lambda 4922$ transitions for a temperature of 20,000 K and an electron density of 10^{16} cm^{-3} . The results displayed in [Figure 3](#) reveal that our simulations can reproduce the overall shape of the line profiles rather well. Also, the fact that we can reproduce both line profiles implies that our theoretical framework is adaptive and can most likely be applied to any transition in the optical. One obvious problem in our simulations is the noise observed in the line wings. This has been traced back to the numerical Fourier transform of the autocorrelation function, resulting from the noise present over long simulation times in the autocorrelation function. We are currently exploring several correction procedures to obtain smoother line profiles.

Our calculations represent the first step towards providing a complete grid of improved line profiles for He I. These will need to be compared in detail with the earlier work of [Beauchamp and Gigosos](#), and eventually included in the calculations of model spectra for DB white dwarfs. Our simulation framework will hopefully permit, in the future, to treat various emitters (such as hydrogen), perturbers, and broadening mechanisms.

References

- Baranger, M. 1962, *Pure and Applied Physics*, 13, 493
 Barnard, A.J., Cooper, J., & Shamey, L.J. 1969, *Astronomy and Astrophysics*, 1, 28
 Beauchamp, A. 1995, *PhD thesis, Université de Montréal*
 Beauchamp, A., Wesemael, F., & Bergeron, P. 1997, *Astrophysical Journal Supplement Series*, 108, 559
 Genest-Beaulieu, C., & Bergeron, P. 2019, *Astrophysical Journal*, 882, 106
 Gigosos, M. A. 2014, *Journal of physics D: Applied Physics*, 47
 Gigosos, M. A. & González, M. Á. 1996, *J. Phys. B: At. Mol. Opt. Phys.*, 29
 Gigosos, M. A. & González, M. Á. 2009, *Astronomy and Astrophysics*, 503, 1
 Griem, H. R. 1974, *Spectral Line Broadening by Plasmas*, (New York: Academic)
 Hegerfeldt, G. C. & Kesting, V. 1988, *APS*, 37, 5
 Hooper, C. F. 1968, *Physical Review*, 165, 1
 Lara, N., González, M. Á., & Gigosos, M. A. 2012, *Astronomy and Astrophysics*, 542, A75